



CHORUS

This is the accepted manuscript made available via CHORUS. The article has been published as:

Strongly gapped spin-wave excitation in the insulating phase of NaOsO_3

S. Calder, J. G. Vale, N. Bogdanov, C. Donnerer, D. Pincini, M. Moretti Sala, X. Liu, M. H. Upton, D. Casa, Y. G. Shi, Y. Tsujimoto, K. Yamaura, J. P. Hill, J. van den Brink, D. F. McMorrow, and A. D. Christianson

Phys. Rev. B **95**, 020413 — Published 23 January 2017

DOI: [10.1103/PhysRevB.95.020413](https://doi.org/10.1103/PhysRevB.95.020413)

Strongly Gapped Spin-Wave Excitation in the Insulating Phase of NaOsO_3

S. Calder,^{1,*} J. G. Vale,^{2,3,†} N. Bogdanov,⁴ C. Donnerer,² M. Moretti Sala,⁵ X. Liu,^{6,7} M. H. Upton,⁸ D. Casa,⁸ Y. G. Shi,^{9,10} Y. Tsujimoto,¹¹ K. Yamaura,^{10,12} J. P. Hill,⁶ J. van den Brink,⁴ D. F. McMorrow,² and A. D. Christianson^{1,13}

¹*Quantum Condensed Matter Division, Oak Ridge National Laboratory, Oak Ridge, Tennessee 37831, USA*

²*London Centre for Nanotechnology and Department of Physics and Astronomy, University College London, Gower Street, London, WC1E 6BT, United Kingdom*

³*Laboratory for Quantum Magnetism, Ecole Polytechnique Fédérale de Lausanne (EPFL), CH-1015, Switzerland*

⁴*Institute for Theoretical Solid State Physics, IFW Dresden, D01171 Dresden, Germany*

⁵*European Synchrotron Radiation Facility, BP 220, F-38043 Grenoble Cedex, France*

⁶*Condensed Matter Physics and Materials Science Department, Brookhaven National Laboratory, Upton, NY 11973, USA*

⁷*Beijing National Laboratory for Condensed Matter Physics and Institute of Physics, Chinese Academy of Sciences, Beijing 100190, China*

⁸*Advanced Photon Source, Argonne National Laboratory, Argonne, Illinois 60439, USA*

⁹*Institute of Physics, Chinese Academy of Sciences, 100190 Beijing, China.*

¹⁰*Superconducting Properties Unit, National Institute for Materials Science, 1-1 Namiki, Tsukuba, 305-0044 Ibaraki, Japan.*

¹¹*International Center for Materials Nanoarchitectonics (MANA),*

National Institute for Materials Science, Tsukuba, Ibaraki 305-0044, Japan.

¹²*JST, Transformative Research-Project on Iron Prinitides (TRIP), 1-1 Namiki, Tsukuba, 305-0044 Ibaraki, Japan.*

¹³*Department of Physics and Astronomy, University of Tennessee, Knoxville, TN 37996, USA*

NaOsO_3 hosts a rare manifestation of a metal-insulator transition driven by magnetic correlations, placing the magnetic exchange interactions in a central role. We use resonant inelastic x-ray scattering to directly probe these magnetic exchange interactions. A dispersive and strongly gapped (58 meV) excitation is observed indicating appreciable spin-orbit coupling in this $5d^3$ system. The excitation is well described within a minimal model Hamiltonian with strong anisotropy and Heisenberg exchange ($J_1=J_2=13.9$ meV). The observed behavior places NaOsO_3 on the boundary between localized and itinerant magnetism.

PACS numbers: 71.30.+h, 75.25.-j

The underlying mechanisms driving a metal-insulator transition (MIT) is an enduring focus of condensed matter physics¹. Recent interest has extended investigations to $5d$ -based transition metal oxides that host new paradigms of competing interactions creating novel MITs². For example spin-orbit coupling (SOC) in $5d^5$ iridates dramatically influences the electronic ground state to allow even the presence of the reduced on-site Coulomb interaction (U) to drive a relativistic Mott MIT³. Conversely, in $5d^3$ osmium-based compounds MITs occur that cannot be reconciled with the reduced U in $5d$ systems, even when the large SOC is taken into account. These compounds therefore fall outside the Mott approximation. Of particular interest in this regard are the osmates NaOsO_3 and $\text{Cd}_2\text{Os}_2\text{O}_7$ which undergo a MIT that is continuous and coincident with the onset of magnetic order indicating the central role of magnetic interactions in the transition⁴⁻⁷. Accessing the collective role of the competing inter and intra-ion electron-electron interactions, SOC and magnetism in driving the MIT is required to gain an understanding of the novel MITs in these osmates.

Outside of a Mott MIT several other mechanism exist to describe the transition, including an Anderson MIT driven by disorder⁸ and a Peirels MIT driven by a structural distortion in a low dimensional system⁹. Slater considered a route in which magnetism could drive a MIT

with the central observation being that within a magnetically ordered system the potential created by an up-spin is different from that created by a down-spin¹⁰. By this definition three-dimensional magnetic ordering with oppositely aligned spins is a route to a MIT, and implicitly includes $q=0$ antiferromagnetic structures. NaOsO_3 exhibits several features consistent with Slater's general scenario^{6,7,11-15}. The MIT occurs concomitant with the onset of antiferromagnetic ordering ($T_N = T_{\text{MIT}} = 410$ K) that can create a periodic potential. Furthermore in NaOsO_3 the MIT is continuous and no structural symmetry change occurs. However several important questions have so far remained experimentally inaccessible hindering the development of further insight into the mechanism of this unusual MIT and prohibiting a quantitative description beyond the mean-field approach invoked by Slater for a magnetic MIT.

Principally, since the MIT is driven by magnetic ordering the magnetic exchange interactions (J) are central to the creation of the MIT in NaOsO_3 . Therefore measuring the dominant exchange pathways and interactions is required to build robust models of the MIT. Additionally the energy scales of the interactions that are required to describe the electronic behavior, such as crystal field splitting, Hund's coupling and SOC have not been accessed. In particular the nominal $5d^3$ electronic occupancy suggests zero orbital angular momen-

tum in the $L-S$ coupling limit and previous experimental descriptions did not require the inclusion of strong SOC. However, mounting experimental evidence in other $5d^3$ systems indicates SOC is required to describe the magnetism^{16–18}. To answer these questions we performed resonant inelastic x-ray scattering (RIXS) to directly probe the $5d$ electrons of the Os ion in NaOsO_3 .

RIXS measurements at the Os L_3 -edge (10.87 keV) were performed on the ID20 spectrometer at the ESRF, Grenoble. A single crystal of NaOsO_3 , space group $Pnma$, was oriented with the (H0L) plane normal to the sample surface. The scattering plane and incident photon polarization were both horizontal. The incident beam was focused to a size of $20 \times 10 \mu\text{m}^2$ (H \times V) at the sample position. Measurements were performed with low ($\Delta E=275$ meV) and high resolution ($\Delta E = 46$ meV) set-ups by switching between a Si(311) channel-cut secondary monochromator and a (664) four-bounce, respectively. Both set-ups used a Si(664) diced spherical analyzer at 2m radius from the detector. Preliminary measurements were performed at the Advanced Photon Source (APS) on the MERIX instrument using an identical set-up to that described in Ref. 18.

We begin by considering the results using the low resolution set-up ($\Delta E=275$ meV) before focusing on our main finding of a spin-wave excitation with high resolution measurements ($\Delta E = 46$ meV). A RIXS map of the orbital excitations, that involve intra or inter $d-d$ transitions, in NaOsO_3 obtained by measuring the inelastic energy loss spectrum at several fixed incident energies through the Os L_3 resonant edge is shown in Fig. 1(a) at 300 K. Three broad inelastic features are observed, labeled E_B , E_C and E_D . On a qualitative level the excitations appear analogous to RIXS measurements on $5d^3$ -based $\text{Cd}_2\text{Os}_2\text{O}_7$ ¹⁸ and exhibit notable differences from measurements of $5d^5$ based iridates¹⁹. The incident energy dependence of features E_B and E_C in the RIXS map is consistent with a nominal splitting of the $5d$ manifold into states with t_{2g} and e_g symmetry with the scattering following dipole selection rules ($\Delta S = 1$). E_B involves intra- t_{2g} transitions whereas E_C is due to t_{2g} - e_g excitations. We assign excitation E_D to ligand-metal charge transfer (LMCT).

The inelastic excitation E_B is centered at 1.27(2) eV and corresponds to intra- t_{2g} transitions. As shown in the inset of Fig. 1(b) even when measured with the high-resolution RIXS set-up E_B remained as a broad single-peaked excitation, significantly broader than the instrumental resolution of 46 meV. This makes any splitting of the t_{2g} manifold from SOC or a structural distortion unresolvable in NaOsO_3 . This contrasts to the case of the iridium-based relativistic Mott insulators, where SOC strongly splits the t_{2g} electronic ground state into $J_{\text{eff}}=1/2$ and $J_{\text{eff}}=3/2$ bands and results in a measured splitting of E_B ^{19,20}. Since E_B consists of intra- t_{2g} transitions we follow the reasoning outlined in Ref. 18 to experimentally define the Hund's coupling energy (J_H) value in NaOsO_3 as $J_H=1.27 \text{ eV}/3.75=0.34 \text{ eV}$ based on the cen-

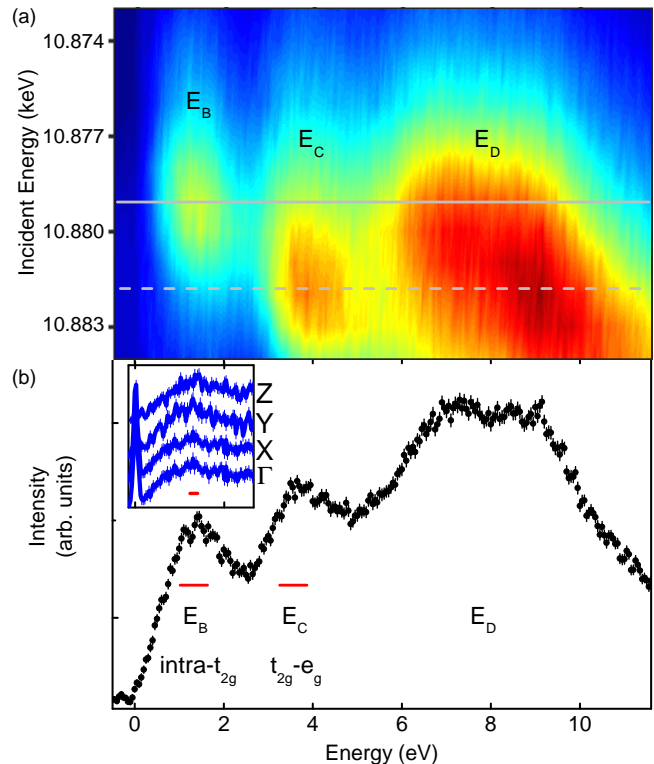


FIG. 1. (a) Excitations measured in NaOsO_3 at various fixed incident energies through the Os L_3 -edge using RIXS. Three inelastic peaks are observed labeled E_B , E_C and E_D . The solid (dashed) gray line indicates the incident energy that yields the maximum intensity for E_B (E_C). (b) RIXS measurement at fixed incident energy of 10.88 keV. Main panel was measured with a resolution of $\Delta E=275$ meV and the inset data was collected with $\Delta E=46$ meV. The horizontal red lines indicate the FWHM experimental resolution. Measurements were performed at 300 K.

ter of E_B . The 3.75 factor derives from the consideration of E_B as consisting of eight $S=1/2$ states, five of which have relative energy $3J_H$ and three having $5J_H$ yielding an average of $3.75J_H$. We note that since any underlying splitting of E_B is unresolved this is an approximate measurement of J_H , however is useful for comparing with similar $5d^3$ systems such as $\text{Cd}_2\text{Os}_2\text{O}_7$.

Excitation E_C is located at 3.6(1) eV and is a direct measure of the crystal field splitting. NaOsO_3 and $\text{Cd}_2\text{Os}_2\text{O}_7$ have a similar local OsO_6 octahedral environment, however the t_{2g} - e_g splitting is 0.9 eV lower in NaOsO_3 ¹⁸. This indicates that considerations beyond the local $5d$ octahedral environment are crucial, which is in line with expectations of the importance of the spatially extended $5d$ orbitals.

The magnetic order and consequently the magnetic exchange interactions are central to the creation of the MIT in NaOsO_3 . Therefore measuring and modeling the dominant exchange pathways is required to yield a complete picture of the MIT. The crystal size of NaOsO_3 is cur-

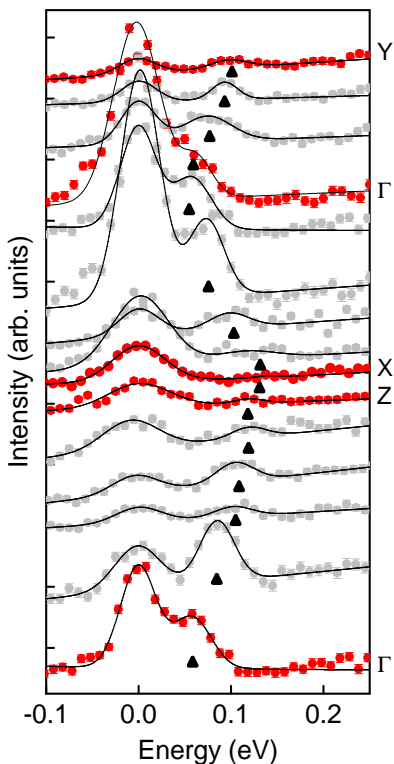


FIG. 2. RIXS measurements of NaOsO₃ at 300 K along high symmetry directions in the Brillouin zone. The line shows the fit to the elastic and inelastic scattering at E_A, with the position of E_A indicated by the triangles. The data have been offset to aid comparison. The strong variation of the elastic line intensity is due to moving through the ideal $2\theta=90^\circ$ RIXS condition where elastic scattering is suppressed.

rently beyond the limits of inelastic neutron scattering, however RIXS offers a route to quantitatively probe the collective magnetic excitations in $5d$ systems¹⁹. The low energy scattering for NaOsO₃ using high resolution Os RIXS is shown in Fig. 2. Measurements along high symmetry directions shows a single resolution limited inelastic excitation (E_A). The excitation, along with the elastic line, were fit with a Gaussian peak shape to follow the dispersion. Fig. 3(a) reveals E_A is strongly dispersive indicative of a spin-wave excitation. The bandwidth is ~ 80 meV with maxima at the zone boundary along the Z and X direction and a reduced energy at Y. A large spin gap of 58 meV is observed at zone center (Γ) that signifies the presence of strong anisotropy in NaOsO₃.

To provide a quantitative description of the magnetic excitations we invoke a minimal model Hamiltonian with nearest neighbor (nn) and next nearest neighbor (nnn) exchange interactions:

$$\mathcal{H} = J_1 \sum_{nn} \mathbf{S}_i \cdot \mathbf{S}_j + J_2 \sum_{nnn} \mathbf{S}_i \cdot \mathbf{S}_j + \Delta \quad (1)$$

A SOC induced anisotropic term is included to account for the gap. For the case of symmetric ex-

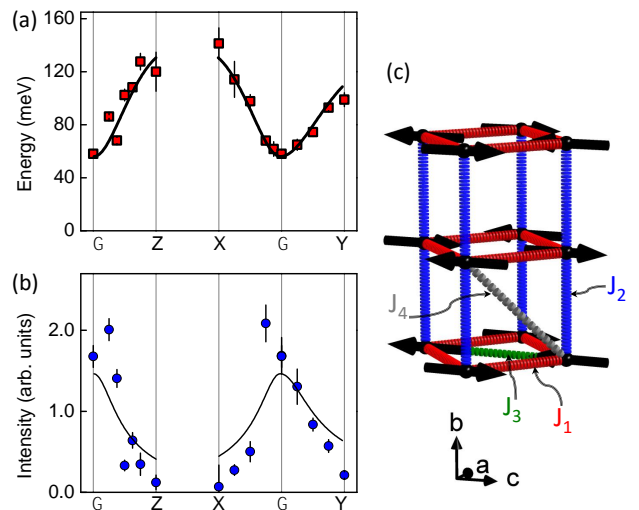


FIG. 3. (a) Measured (squares) and calculated (line) dispersion of E_A along high symmetry directions. (b) Measured (circles) and calculated (line) intensity of E_A. (c) The calculations were performed using equation (1), a minimal model Hamiltonian with the exchange interactions $J_1=J_2=13.9$ meV.

change anisotropy $\Delta = \Gamma \sum_{nn,nnn} S_i^z S_j^z$ and for single-ion anisotropy $\Delta = D \sum (S_z^2)_i$

The RIXS data for NaOsO₃ was modeled within a linear spin wave (LSW) approximation²¹ and the results checked against numerical calculations using SpinW²². The nominal spin-only value of $S=3/2$ was used throughout. Fitting the experimental dispersion to equation (1) produces close agreement to both the dispersion and corresponding intensity, Fig. 3, indicating the minimal model Hamiltonian captures the essential features and consequently provides an experimental assignment of the dominant magnetic exchange interactions and their energy. The fitting yields $J_1=J_2=13.9(5)$ meV and $\Gamma=1.4(1)$ meV. Allowing J_1 and J_2 to vary independently did not improve the fit, reflecting the pseudo-cubic nature of the structure. Adding a third-nearest neighbor term J_3 , or $J_3=J_4$ to recover the cubic limit, alters the energy at Z with respect to X, however within resolution the measured energy at $X=Z$. Therefore we conclude that exchange interactions J_3 and above have a magnitude appreciably less than J_1 or J_2 and limit the Hamiltonian to equation (1). Consequently NaOsO₃ is well described by dominant nearest neighbor magnetic interactions in three dimensions forming a robust G-type antiferromagnetic order in this perovskite. Replacing exchange anisotropy with a single-ion anisotropy ($D \sum (S_z^2)_i$) term yields the same J_1 and J_2 values and $D=4$ meV.

The mechanism for the spin-gap is effectively disconnected from the magnetic exchange interactions in equation (1). However, the presence of such a large spin-gap is significant in terms of the underlying physics in NaOsO₃. In particular, all possible mechanisms to open a spin-gap, single-ion anisotropy (SIA), the Dzyaloshinskii-

Moriya (DM) interaction and exchange anisotropy, require SOC. We briefly consider how the anisotropies influence NaOsO₃. SIA arises due to a non-cubic environment and in NaOsO₃ the OsO₆ octahedra are weakly trigonally and tetragonally compressed. However, such a large gap due to SIA does not appear consistent with the reduced spin-gaps of 15-20 meV observed in other 5d³ osmates with similar distortions¹⁷. In NaOsO₃ a non-zero local DM vector exists since the oxygen mediating the superexchange interaction between the two Os sites does not sit at an inversion center. Experimentally there is evidence of weak ferromagnetism²³, however the spin-canting producing this was undetectable with neutron diffraction⁷. This would suggest that the DM interaction, while present, is weak to first order. Exchange anisotropy, a pseudodipolar effect, results as a consequence of second-order SOC effects between neighboring Os ions, and hence is generally weaker than the DM interaction and SIA. However, in 5d systems the extended orbitals result in enhanced collective behavior within the lattice compared to, for example, that which occurs in 3d transition metal oxides. Indeed this was shown in NaOsO₃ with the observation of a record large spin-phonon shift at the MIT due to the extended Os orbitals¹⁵.

The measurement of a large-spin gap indicates that SOC is required in a complete description of NaOsO₃. The magnitude of SOC scales with the atomic number, therefore in 5d³ osmates it is comparable to 5d⁵ iridates. However, when describing the properties of NaOsO₃ the role of SOC has only been required to be included as a perturbation^{6,7,11-15}. Conversely for 5d⁵ iridates SOC is necessary to describe both magnetism and the insulating state. This has created an apparent dichotomy between the effect of SOC, particularly when considering the divergent electronic ground states indicated from the RIXS spectra between 5d³ and 5d⁵. A first approximation is that the altered electronic occupancy causes an increased Hund's coupling in 5d³ systems favoring a quenching of orbital momentum. However, the broad scattering observed for E_B in Fig. 1 indicates underlying splitting of the t_{2g} orbitals, either through structural distortions or SOC or a combination of both. One consequence of an increased role of SOC in NaOsO₃ was considered theoretically to reduce the effective U and place the system closer to the itinerant limit description of magnetism²⁴. However, the agreement of the minimal-model Hamiltonian, based on localized spins, to the RIXS spectra would suggest that the behavior of NaOsO₃ appreciably departs from being fully itinerant. Indeed this would be expected even within the mean-field Hartree-Fock description used by Slater to describe a magnetic MIT since at the transition local moments are necessarily formed²⁵. While in a pure Slater description this would be treated by self-consistent single electron theory, at least to a good approximation the behavior can be described by a Heisen-

berg model and places NaOsO₃ on the boundary between local-moment and itinerant magnetism.

The strongly dispersing excitation in NaOsO₃ contrasts with the dispersionless excitation of Cd₂Os₂O₇ observed previously with RIXS¹⁸. The use of an Ising-like description to describe Cd₂Os₂O₇ and a Heisenberg model to capture the behavior for NaOsO₃ may indicate distinct magnetic interactions in these two closely related materials. While the behavior appears to diverge, indicating the potential for varied and exotic phenomena in related 5d³ oxides, for both osmates the magnetic excitation spectra reveal an appreciable influence of SOC.

The 5d orbital and collective magnetic excitations in NaOsO₃ have been probed with RIXS. Well-defined spin waves were observed and described within linear spin wave theory using a minimal model Hamiltonian that captured the essential features. Nearest and next nearest neighbor Heisenberg exchange interactions of $J_1=J_2=13.9$ meV were found to describe the dispersion, indicating strong three-dimensional magnetic interactions. The presence of significant anisotropy in the system was observed with the measurement of a large spin gap of 58 meV. This is a direct consequence of intrinsically strong SOC in this 5d compound, however the role of SOC on the ground state departs from 5d⁵ iridates. In terms of the mechanism of the MIT the results support a three-dimensional magnetically driven route, consistent with the general scenario proposed by Slater. The Hamiltonian presented here provides the magnetic interaction energy scales and their pathways required to describe the MIT. Moreover, the presence of SOC and the influence this has within a system with extended orbitals and strong hybridization has to be considered as playing an important role when considering the collective interactions and the MIT.

ACKNOWLEDGMENTS

A. D. C. thanks A. Taylor for useful discussions. We thank C. Henriquet and R. Verbeni at the ESRF for design and manufacture of the high-temperature stage. Preliminary measurements were performed at 9-ID-B and 30-ID (MERIX), APS, which is a U.S. Department of Energy (DOE) Office of Science User Facility operated for the DOE Office of Science by Argonne National Laboratory under Contract No. DE-AC02-06CH11357. The research at ORNL was sponsored by the Scientific User Facilities Division, Office of Basic Energy Sciences, U.S. Department of Energy. Work in London was supported by EPSRC. J. G. V. would like to thank UCL and EPFL for financial support via a UCL Impact Studentship. X. L. acknowledges financial support from MOST (No. 2015CB921302) and CAS (No. XDB07020200) of China.

- * caldersa@ornl.gov
† j.vale@ucl.ac.uk
- ¹ M. Imada, A. Fujimori, and Y. Tokura, *Rev. Mod. Phys.* **70**, 1039 (1998).
 - ² W. Witczak-Krempa, G. Chen, Y. B. Kim, and L. Balents, *Annual Review of Condensed Matter Physics* **5**, 57 (2014).
 - ³ B. J. Kim, H. Ohsumi, T. Komesu, S. Sakai, T. Morita, H. Takagi, and T. Arima, *Science* **323**, 1329 (2009).
 - ⁴ D. Mandrus, J. R. Thompson, R. Gaal, L. Forro, J. C. Bryan, B. C. Chakoumakos, L. M. Woods, B. C. Sales, R. S. Fishman, and V. Keppens, *Phys. Rev. B* **63**, 195104 (2001).
 - ⁵ J. Yamaura, K. Ohgushi, H. Ohsumi, T. Hasegawa, I. Yamauchi, K. Sugimoto, S. Takeshita, A. Tokuda, M. Takata, M. Udagawa, M. Takigawa, H. Harima, T. Arima, and Z. Hiroi, *Phys. Rev. Lett.* **108**, 247205 (2012).
 - ⁶ Y. G. Shi, Y. F. Guo, S. Yu, M. Arai, A. A. Belik, A. Sato, K. Yamaura, E. Takayama-Muromachi, H. F. Tian, H. X. Yang, J. Q. Li, T. Varga, J. F. Mitchell, and S. Okamoto, *Phys. Rev. B* **80**, 161104 (2009).
 - ⁷ S. Calder, V. O. Garlea, D. F. McMorrow, M. D. Lumsden, M. B. Stone, J. C. Lang, J.-W. Kim, J. A. Schlueter, Y. G. Shi, K. Yamaura, Y. S. Sun, Y. Tsujimoto, and A. D. Christianson, *Phys. Rev. Lett.* **108**, 257209 (2012).
 - ⁸ P. W. Anderson, *Phys. Rev.* **109**, 1492 (1958).
 - ⁹ R. E. Peierls, *Quantum Theory of Solids* (Oxford University Press, New York, 1955).
 - ¹⁰ J. C. Slater, *Phys. Rev.* **82**, 538 (1951).
 - ¹¹ Y. Du, X. Wan, L. Sheng, J. Dong, and S. Y. Savrasov, *Phys. Rev. B* **85**, 174424 (2012).
 - ¹² M.-C. Jung, Y.-J. Song, K.-W. Lee, and W. E. Pickett, *Phys. Rev. B* **87**, 115119 (2013).
 - ¹³ I. L. Vecchio, A. Perucchi, P. Di Pietro, O. Limaj, U. Schade, Y. Sun, M. Arai, K. Yamaura, and S. Lupi, *Scientific Reports* **3**, 2990 (2013).
 - ¹⁴ S. Middey, S. Debnath, P. Mahadevan, and D. D. Sarma, *Phys. Rev. B* **89**, 134416 (2014).
 - ¹⁵ S. Calder, J. H. Lee, M. B. Stone, M. D. Lumsden, J. C. Lang, M. Feyngenson, Z. Zhao, J.-Q. Yan, Y. G. Shi, Y. S. Sun, Y. Tsujimoto, K. Yamaura, and A. D. Christianson, *Nature Communications* **6**, 8916 (2015).
 - ¹⁶ E. Kermarrec, C. A. Marjerrison, C. M. Thompson, D. D. Maharaj, K. Levin, S. Kroecker, G. E. Granroth, R. Flacau, Z. Yamani, J. E. Greedan, and B. D. Gaulin, *Phys. Rev. B* **91**, 075133 (2015).
 - ¹⁷ A. E. Taylor, R. Morrow, R. S. Fishman, S. Calder, A. I. Kolesnikov, M. D. Lumsden, P. M. Woodward, and A. D. Christianson, *Phys. Rev. B* **93**, R220408 (2016).
 - ¹⁸ S. Calder, J. G. Vale, N. A. Bogdanov, X. Liu, C. Donnerer, M. H. Upton, D. Casa, A. H. Said, M. D. Lumsden, Z. Zhao, J. Q. Yan, D. Mandrus, S. Nishimoto, J. van den Brink, J. P. Hill, D. F. McMorrow, and A. D. Christianson, *Nature Communications* **7**, 11651 (2016).
 - ¹⁹ J. Kim, D. Casa, M. H. Upton, T. Gog, Y.-J. Kim, J. F. Mitchell, M. van Veenendaal, M. Daghofer, J. van den Brink, G. Khaliullin, and B. J. Kim, *Phys. Rev. Lett.* **108**, 177003 (2012).
 - ²⁰ M. Moretti Sala, S. Boseggia, D. F. McMorrow, and G. Monaco, *Phys. Rev. Lett.* **112**, 026403 (2014).
 - ²¹ Diagonalizing the Hamiltonian in equation (1) within a LSW approximation gives the spin wave energy ω : $\omega = S\sqrt{D - X - Y}$, where $D = 36\Delta^2 + 48\Delta J_1 + 24\Delta J_2 + 12J_1^2 + 2J_2^2 + 16J_1 J_2$, $X = 4J_1^2 \cos 2\pi h + 2J_2^2 \cos 2\pi h + 4J_1^2 \cos 2\pi l$, $Y = 2J_1^2 \cos [2\pi(h-l)] + 2J_2^2 \cos [2\pi(h+l)] + 16J_1 J_2 \cos \pi h \cos \pi k \cos \pi l$. In a similar fashion the intensity can be expressed by: $S(q, \omega) = S \left[\frac{D - (X - Y)}{D - (X + Y)} \right] \delta(\omega, \omega_q)$.
 - ²² S. Toth and B. Lake, *Journal of Physics: Condensed Matter* **27**, 166002 (2015).
 - ²³ Y. G. Shi, Y. F. Guo, S. Yu, M. Arai, A. A. Belik, A. Sato, K. Yamaura, E. Takayama-Muromachi, H. F. Tian, H. X. Yang, J. Q. Li, T. Varga, J. F. Mitchell, and S. Okamoto, *Phys. Rev. B* **80**, 161104 (2009).
 - ²⁴ B. Kim, P. Liu, Z. Ergonenc, A. Toschi, S. Khmelevskiy, and C. Franchini, arXiv:1601.03310 (2016).
 - ²⁵ F. Gebhard, *The Mott Metal-Insulator Transition* (Springer, Berlin, 1997).